Growth and Labelling of Cell Wall Components of the Brown Alga *Ectocarpus* in Microfluidic Chips

Bénédicte Charrier[1]*[†], Samuel Boscq[1], Bradley J. Nelson[2] and Nino F. Läubli[2,3]*[†]

[1] *Modeling and Morphogenesis of Macroalgae, UMR 8227, CNRS – Sorbonne University, Marine Biological Station, Roscoff, France,* [2] *Multi-Scale Robotics Lab, ETH Zürich, Zurich, Switzerland,* [3] *Molecular Neuroscience Group, University of Cambridge, Cambridge, United Kingdom*

Polydimethylsiloxane (PDMS) chips have proven to be suitable environments for the growth of several filamentous organisms. However, depending on the specimen, the number of investigations concerning their growth and cell differentiation is limited. In this work, we monitored the developmental pattern of the brown alga *Ectocarpus* inside PDMS lab-on-chips. Two main methods of inoculation of the lab-on-chip were tested, i.e., *via* the direct injection of spores into the chamber as well as through the insertion of sporophyte filaments. The resulting growth rate, growth trajectory, cell differentiation, and cell branching were monitored and quantified for 20 days inside 25 or 40 μm parallel channels under standard light and temperature conditions. With growth rates of 2.8 μm$\cdot$h^{-1}, normal growth trajectories and cell differentiation, as well as branching occurring inside the microfluidic environment, the main development steps were shown to be similar to those observed in non-constrained *in vitro* conditions. Additionally, the labelling of *Ectocarpus* cell wall polysaccharides using calcofluor for cellulose detection and immunolocalisation with monoclonal antibodies for alginates showed the expected patterns when compared to open space growth evaluated with either epifluorescence or confocal microscopy. Overall, this article describes the experimental conditions for observing and studying the basic unaltered processes of brown algal growth using microfluidic technology which provides the basis for future biochemical and biological researches.

Keywords: microfluidics, brown alga, tip growth, on-chip immunolocalisation, *Ectocarpus*, filaments, lab-on-chips

INTRODUCTION

Because of their highly polarised shape, filamentous organisms tend to raise many questions concerning their growth and differentiation, such as if their growth is restricted to the apical cell, which corresponds to a case of localised growth, or if it is shared by all the cells composing the filament as seen with diffuse growth patterns. Additionally, it is yet to be discovered how the complex intercellular transport of material and the correspondingly required communication in such polarised and uniaxial living structures occur. Furthermore, it is unclear what cues lead to the distribution of cell differentiations along such a linear tissue and how the repetition of all these functions is controlled when architectural complexity is increased through branching.

With advances in microtechnology driving the development of novel microelectromechanical systems (MEMS) and, consequently, the broader availability of corresponding fabrication facilities, the use of lab-on-chip devices has gained increasing interest in many research fields ranging from chemistry and biomedical engineering to biology (Azizipour et al., 2020; Bayareh et al., 2020; Pei et al., 2020; Zhu et al., 2020; Berlanda et al., 2021; Läubli et al., 2021a). As a subset of these technologies, microfluidic devices, i.e., structures containing fluid filled channels with dimensions in the µm to mm range, have been successfully established as a versatile tool that enables new avenues of research through the manipulation and handling of small organisms (Läubli et al., 2021b). In recent years, several pieces of work have relied on microfluidic technologies to study a wide range of organisms through the evolutionary tree including mammalians and plants (Peyrin et al., 2011; Siddique and Thakor, 2013; Tong et al., 2015; Shamsudhin et al., 2016; Burri et al., 2018). The reasons for using microfluidic devices to study small specimens are numerous and reflect the need of investigations to spatially constrain these cultured materials, for example by limiting the height and width of the available environment in the chip path in order to simplify long-term monitoring and improve the resolution of microscopy-based observations (Shamsudhin et al., 2016; Kozgunova and Goshima, 2019; Zhou et al., 2021). It can also allow the separation of filaments which would otherwise grow too densely (Bascom et al., 2016) or guide them to grow perpendicular to a measuring device, such as a force sensor, positioned at the exit of the chip (Burri et al., 2018). Furthermore, depending on their design, constrained paths can also be utilised to evaluate the existence of directional memory of growing filaments (Held et al., 2011). Finally, in addition to the guidance of small organisms, microfluidic chips can be used for automated flows of controlled chemical compounds (Agudelo et al., 2013) as well as combined with microelectrodes to enable the generation of applied electrical pulses (Agudelo et al., 2016), both of which can be perceived as cues for the activation or repression of downstream signalling pathways in living specimens.

Nevertheless, the potential of microfluidic devices must first be evaluated for each biological model to avoid misinterpretations of subsequent results due to unidentified effects induced by the constraining environment. In the protonemata of the moss *Physcomitrium patens*, an initial study demonstrated that growth rate, cell differentiation, protoplast regeneration, and responses to drugs of specimens growing inside microchannels were all comparable to observations from samples under standard growth conditions (Bascom et al., 2016), thereby validating the use of polydimethylsiloxane (PDMS) chips for their study. However, the response to these conditions depends, to some extent, on the geometric parameters of the chip. The available height between the glass slide and the PDMS layer has been shown to impact certain cellular biological processes. When moss protonemata filaments with a diameter of 21 µm were constrained inside channels with a height of 4.5 µm, their microtubule velocity was reduced while the viability and growth of the filaments were not impaired (Kozgunova and Goshima, 2019). On the other hand, growth in maze and grid PDMS meshworks was shown

to significantly impair both the growth rate and the branching pattern of the fungus *Neurospora crassa* (Held et al., 2011), although this effect was attributed to the design of the chip pathways rather than to the PDMS polymer which is generally known to be chemically compatible and non-toxic.

Here, we evaluated the ability of *Ectocarpus* sp. to grow within PDMS-based microfluidic devices and assessed the suitability of our approach for immunocytochemistry in the filamentous brown alga *Ectocarpus* sp. Brown algae (Phaeophyceae) are a class of photo-autotrophic organisms that evolved independently of animals and plants. The ancestor of this kingdom, Stramenopiles, diverged 1.6 billion years ago from the eukaryotic ancestor shared by the animal and plant lineages, i.e., the Opisthokonta and the Archaeplastida, respectively (Baldauf, 2003). Since the knowledge of the first genomic sequence of brown algae (Cock et al., 2010), metabolic, cellular, and developmental studies have confirmed their peculiar phylogenetic position, as they combine animal and plants characteristics (Bothwell et al., 2008; Cock et al., 2010; Michel et al., 2010; Popper et al., 2011; Bogaert et al., 2019; Rabillé et al., 2019a). While *Ectocarpus* was shown to grow on PDMS surfaces immersed in seawater (Evariste et al., 2012), we studied how its filaments cope with the restricted and constrained spatial environment provided by a microfluidic chip. We focused on the prostrate filament of the sporophyte because it grows immediately after mitospore or zygote germination. More importantly, this filament grows by tip growth, a mechanism that is shared by many organisms belonging to other phyla of the eukaryotic evolution tree, thereby, allowing macroevolutive scale comparisons. In addition to the oomycetes belonging to the Stramenopiles like brown algae, tip growing cells include plant pollen tubes and plant root hairs, moss filaments (protonemata) and algal rhizoids of the Archaeplastida phylum, and fungal hyphae and neurons in the Opisthokonta phylum (**Figure 1**). Besides its different evolutionary history, *Ectocarpus* differs from other tip-growing organisms in many ways. Its sporophyte filaments are the slowest tip-growing organisms reported to date with a growth speed of 2.5 µm·h^{-1} (**Figure 1**), *i.e.*, 700 times slower than the pollen tube (Rabillé et al., 2019a), which highlights the necessity of evaluating lab-on-chip technology to simplify their long-term investigation in controlled environments. In addition, we showed that the mechanisms of tip growth selected by this alga relies on an adjustment of its cell wall thickness at the very tip of the apical cell, while most of the other tip growing cells, including the pollen tube, control their growth by varying the cell wall stiffness at this position (Rabillé et al., 2019a). Hence, further studies of tip growth mechanisms in *Ectocarpus*, namely those controlling the cell wall thickness during apical growth, require the development of technologies allowing to simultaneously monitor several filaments growing in similar conditions over a long period of time.

In this technical paper, we designed two PDMS-based lab-on-chips consisting of straight parallel channels to constrain filament growth and to guide them in a single, horizontal direction in contrast to their growth in all directions as observed in open space environments. The healthiness and growth performance of *Ectocarpus* filaments inside these microfluidic environments

FIGURE 1 | Diversity of tip growth in the eukaryotic tree. The phylogenetic position of eukaryotic taxa with tip-growing organisms. The cell shapes and typical growth rates for each organism are shown. Scale bars (from left to right): Archaeplastida, 20, 5, 5, and 5 μm; Opisthokonta, 5 and 5 μm; and Stramenopiles, 5 and 5 μm. Modified from Rabillé et al. (2019a).
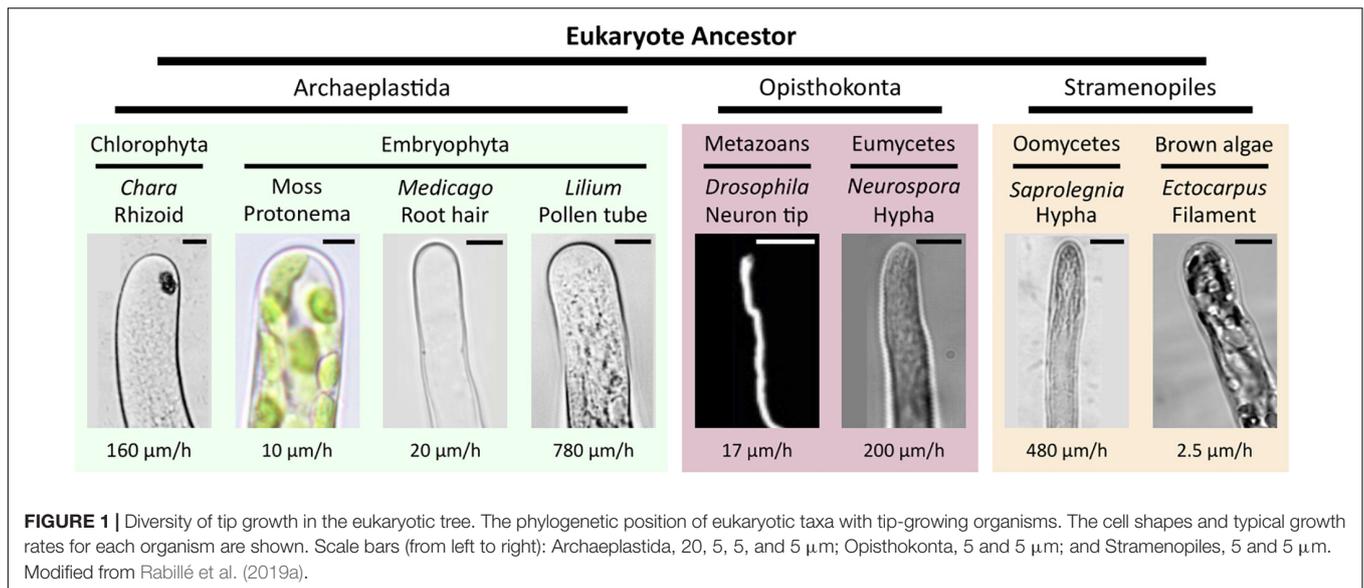
were monitored for up to 20 days and their growth rates were, in addition to the qualitative evaluation of several development steps, quantitatively compared to open space growth conditions. Finally, the ability to label cytological markers, either by immunochemistry or directly with vital dyes, was tested to study the suitability of microfluidic environments for subsequent investigations of the tip growth in the brown alga *Ectocarpus*.

MATERIALS AND METHODS

Chip Design

The transparent polymer PDMS, as often used for the fabrication of microfluidic environments, was shown to be not toxic for the brown algae *Ectocarpus* sp. (Evariste et al., 2012) as blended filaments inoculated on surfaces of different PDMS compositions grew as expected. **Figure 2A** shows a schematic of a PDMS device in side view. The key elements of the structure consist of the inlet, the main chamber, as well as the microchannels. The inlet has a diameter of 1.2 mm and enables filling of the chamber and loading of the samples. The height of the chamber is 100 μm to ensure sufficient availability of nutrients. Depending on the planned experiment, a design with a circular (**Figures 2B,C**) or triangular chamber (**Figures 2D,E**) can be chosen. The chamber is connected to numerous microchannels with a height of 20 μm. The reduction in height from the chamber to the channel constricts the specimen's growth direction and, by that, allows for long-term imaging within a stable focal plane. While circular chambers connect to 44 channels with a width of 25 μm and allow for multiplex observations of the specimens, triangular chambers connected to 14 channels with a width of 40 μm to enable the detailed investigation of specific growth trajectory, e.g., filament undulations. The channels are separated by PDMS walls with a width of 20 μm, which is necessary to ensure proper sealing and adhesion between the PDMS device and the glass substrate. **Figure 2D** shows a schematic of a

PDMS device with a triangular chamber. At the entrance of the channels, a small funnel guides filaments from the chamber into the channel, thereby enhancing the percentage of filaments growing into the channels. Once an entrance or channel is filled, a constriction at the end of the funnel should prevent an additional filament from entering the already occupied channel. Additionally, the constriction reduces the risk of specimens getting flushed through the channels during the initial filling of devices with wider structures.

The width chosen for the channels was a compromise of several criteria. On the one hand, narrower channels would increase the spatial constraints for *Ectocarpus*, which, despite being of broader interested concerning the resulting growth cell response, is not the focus of this initial investigation on the feasibility of lab-on-chip technology. Additionally, narrower channels would require a higher loading pressure, which could damage the samples or even separate the bond between the PDMS structure and the glass substrate. On the other hand, the use of wider channels bares the risk of samples passing through the microchannels rather than being collected in the chamber during loading. Overall, considering biological features as well as manufacturing constraints and technical challenges, we considered 25 μm to be a compromise that would allow the algae to have sufficient nutrients while ensuring a mechanically robust lab-on-chip device.

As to the chamber, its geometry was adjusted to allow a sufficiently large number of connected channels for each design while simultaneously limiting the volume available inside the chamber. Thus, it optimises the chance of obtaining filaments growing parallel to each other inside channels which is a crucial factor for the efficient study of slow-growing organisms like *Ectocarpus*. However, although no direct influence on the specimen's growth was observed in relation to changing the inlet geometry, future studies could examine the impact of additional design parameters, such as the height or diameter of the inlet, on the specimen's health and viability.
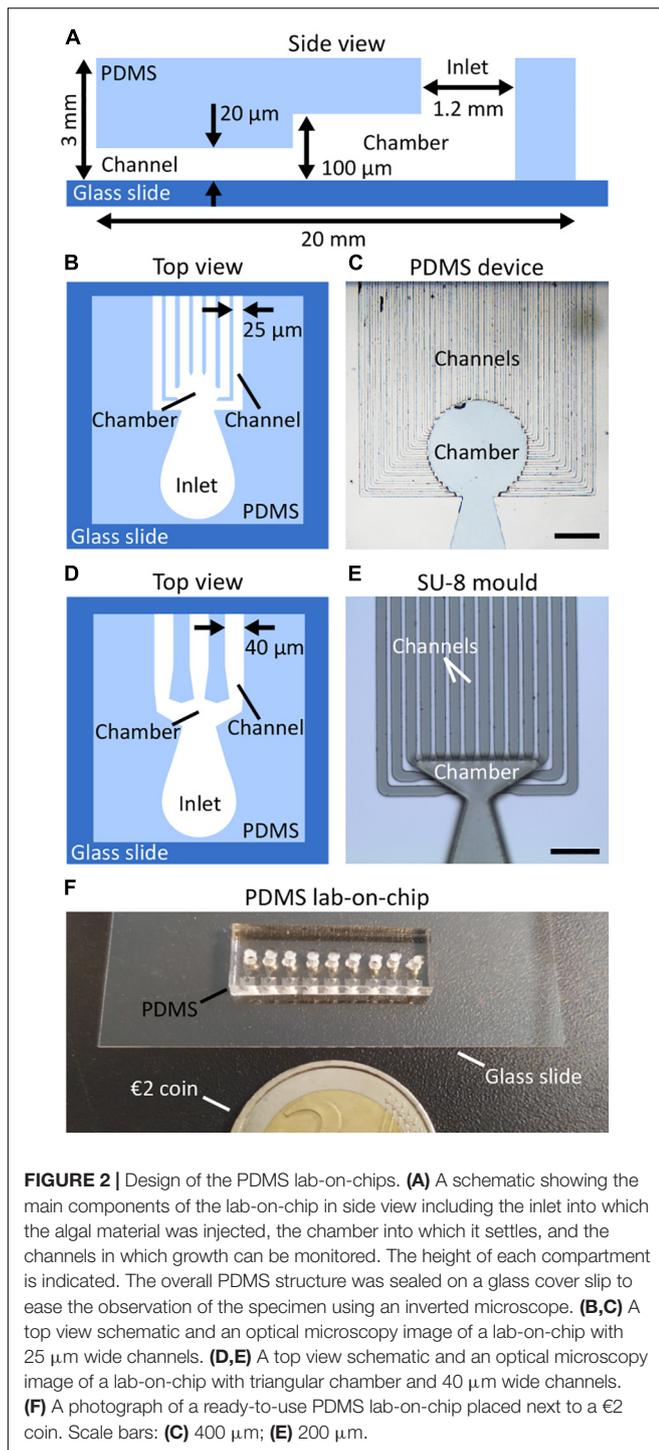
FIGURE 2 | Design of the PDMS lab-on-chips. **(A)** A schematic showing the main components of the lab-on-chip in side view including the inlet into which the algal material was injected, the chamber into which it settles, and the channels in which growth can be monitored. The height of each compartment is indicated. The overall PDMS structure was sealed on a glass cover slip to ease the observation of the specimen using an inverted microscope. **(B,C)** A top view schematic and an optical microscopy image of a lab-on-chip with 25 μm wide channels. **(D,E)** A top view schematic and an optical microscopy image of a lab-on-chip with triangular chamber and 40 μm wide channels. **(F)** A photograph of a ready-to-use PDMS lab-on-chip placed next to a €2 coin. Scale bars: **(C)** 400 μm; **(E)** 200 μm.

Fabrication

The lab-on-chips were fabricated by double-layer photolithography in clean room environments and by mould replication techniques. Silicon wafers were cleaned with acetone, isopropanol, and deionised water prior to mould fabrication. For the layer containing the microchannels, the photosensitive polymer SU-8 3025 (*Kayaku Advanced Materials*)

was spin-coated on the wafers using a three-step process with a maximum angular velocity of 4500 rpm to obtain a uniform photoresist layer of 20 μm. The corresponding design of the channel layer was transferred onto the photoresist using a mask aligner (MA6/BA6, *Süss MicroTec*). Finally, the wafers were developed (mr-Dev 600, *Micro Resist Technology GmbH*) and hard baked at 150°C for 5 min to improve the stability of the channels and their adhesion to the silicon substrate. The second layer of the lab-on-chip, i.e., the elevated section containing the inlets as well as the main chamber, was fabricated through an additional photolithography process using SU-8 100 (*Kayaku Advanced Materials*) and a maximum angular velocity of 3000 rpm to ensure a uniform 100 μm thick layer of photoresist. **Figure 2E** shows an optical microscopy image of a fabricated mould with a triangular chamber to be used for PDMS replication. The observed variation in the focal plane is based on the height difference between the channel layer and the triangular chamber layer.

Prior to PDMS casting, the fabricated structures were vapour coated with (tridecafluoro-1,1,2,2-tetrahydrooctyl) trichlorosilane (CAS 78560-45-9, *ABCR*) and heated to 120° C for 10 min to improve the reusability of the mould. PDMS (Sylgard 184, *Dow Corning*) with a weight ratio of 1:10 (curing agent to pre-polymer) was mixed sufficiently for 5 min, poured over the SU-8 mould, and degassed for 30 min in a vacuum chamber. To transfer the 3D pattern into the polymer, the PDMS was cured for 1 h in an oven at 80°C. Finally, the PDMS was cut and peeled off the mould and the inlets were punched using a biopsy punch with a diameter of 1.5 mm (BP15, *Vetlab*). To chemically bond the PDMS and the cover glass with a thickness of 0.17 μm, both surfaces were exposed to oxygen plasma (Femto Plasma Asher, *Diener Electronics*) for 30 s before being brought in contact. Slight pressure was manually applied to ensure proper contact between the entirety of the lab-on-chip and the cover glass to prevent future algal specimens from growing beyond the dimensions of the corresponding microchannels.

For size comparisons, **Figure 2F** shows a ready-to-use lab-on-chip with 25 μm wide channels next to a €2 coin.

Sterilisation of the Chips

The chips were sterilised by UV irradiation for 30 min in a sterile laminar flow hood. Then, they were used either dry or pre-filled with sterile seawater (see below).

Ectocarpus Cultivation

Ectocarpus strain CCAP 1310/4 (also named Ec32) from the Culture Collection of Algae and Protozoa was grown in natural seawater (approximately 550 mosmoles) supplemented by vitamins and microelements as described by Le Bail and Charrier (2013). Sporophyte filaments were produced from the germination of swimming mitospores (Charrier et al., 2008). Cultivation took place at 13°C under 12:12 light:dark conditions (light intensity of approximately 29 μE m^{-2} s^{-1}), usually on the main types of plastic and glassware. Seawater was renewed every 2 weeks when algae were grown in open space environments.

On-Chip Inoculation
Optimisation of the Loading Procedure
The 1.2 mm diameter inlet was filled with seawater by applying a constant pressure *via* a pipette mounted with a cut pipette tip to seal the 1.2 mm inlet.

As seawater is 1.3% more viscous and has a higher surface tension than pure water, filling the channels can be more difficult. Consequently, if the applied pressure is too low, the seawater introduced into the inlet only fills the chamber but not the channels (**Supplementary Figures 1A,B**). A solution of seawater stained with bromophenol blue was used to optimise the channel filling procedure with a micropipette. Once the protocol was established, algal material was introduced into the chamber.

Channel Filling
The algal material was introduced into the chamber by applying a steady pressure high enough to bring the algal material just at the entrance of the channels, yet low enough to prevent the algae from being flushed out of the chamber. After inoculation, the material was left still for 2 h to allow the spores to attach to the chamber surface and the glass substrate. If sporophytes were used instead of spores, they were removed after 2 h. The channels were then filled with seawater by applying a pipetting pressure high enough to allow the liquid to move from the chamber to the channels. Because we did not use a pump with standardised equipment (e.g., pipe diameter), the numerical value of the pressure is not known. However, pressure required to fill the channel when pressing on a micropipette has been experienced previously using blue seawater as a visible coloured marker to monitor channel filling (**Supplementary Figure 1C**). It is also worth noting that the required pressure varied slightly between each structure, as, due to their manual preparation, the final length of the microchannels showed minor variations. To confirm complete filling of the channels with clear seawater, the channels outlets were monitored under a microscope for the release of air bubbles. Channels in which air remained trapped after the first filling procedure (as shown in **Supplementary Figure 1D**) were flushed several times.

Once inoculated, the lab-on-chip was transferred to a Petri dish filled with seawater and kept fully submerged. It was cultured under standard conditions as described above, thereby, allowing for comparisons to open space cultivations. Seawater was renewed every 2 days. No salt crystals were observed inside the channels during at least 3 weeks.

This procedure was repeated on 7 independent experiments summing 12 slides containing a total of 108 lab-on-chip devices. Altogether, more than 500 filaments were observed.

It is important to highlight that the described on-chip inoculation has been tested with regards to the loading procedure and, consequently, to the optimum location for the loaded material to ensure successful germination and improved specimen health. The optimised method, as described above, relies on a two-step filling process for the microfluidic device in which loaded fertile sporophytes or released spores were initially prevented from entering the channels by the liquid/air interface formed between the chamber and the channel. The channels were then made accessible to the germinating spores by flushing the full structure.

In contrast, filling the chamber as well as the channels with fertile sporophytes or spores in a single step did not only lead to partially blocked channels due to broken or small filament pieces (**Supplementary Figure 2A**) but further allowed the still swimming spores to enter the channels. This led to severely impaired filament growth behaviours with delayed spore germinations and qualitatively less asymmetrical cell divisions. Furthermore, some cases demonstrated growth directions perpendicular to the channel axis (**Supplementary Figure 2B**) as well as a general reduction in growth rate with less pronounced cell growth of the apical cells and shorter filaments (**Supplementary Figure 2C**). Finally, while cell rounding was still observed for filaments with normal apical growth (**Supplementary Figure 2D**), branching has not been detected for any spores that initially germinated inside the channels.

As a suitable alternative allowing many channels to be filled with branches at a similar stage of development (**Supplementary Figure 2E**), the loading of non-fertile sporophytes into fully flushed structures can be proposed. As *Ectocarpus* development is reiterative, subsequent branch growth followed the same developmental process as for primary filaments while the spore germination and initial asymmetrical divisions were skipped.

Image Acquisition
The Leica DMI-8 inverted microscope was used to observe calcofluor (Ex/Em: 380/475 nm) and fluorescein isothiocyanate (FITC; Ex/Em: 495/520 nm) labelling with the corresponding filters. Confocal microscopy (TCS SP5 AOBS inverted confocal microscope, *Leica, objective Plan-Apochromat 63×/1.4 Oil*) was used to increase the z spatial resolution compared to image acquisition by epifluorescence microscopy.

Labelling of Cellular Components
Cellulose was stained by incubating the lab-on-chip in 0.01% calcofluor white solution (fluorescent brightener 28, F-3543, *Sigma-Aldrich*) for 30 min at room temperature (RT) in the dark. The solution was injected into the channels by high pressure pipetting. Observation was performed under UV light using epifluorescence microscopy after flushing the channels with fresh seawater at least twice and after incubation for at least 15 min at RT between each rinsing step.

Immunolocalisation of cell wall polysaccharides in the lab-on-chip was developed by adapting the protocol from Rabillé et al. (2019b). The main modification consisted in fixing the algal material in 4% paraformaldehyde prepared in H_2O instead of seawater. All the solutions were rinsed by high pressure pipetting into the inlet which occasionally resulted in the loss of some filaments.

Statistical Evaluation
Statistical evaluations concerning the specimens' growth rates were performed as double-sided t-test with unequal variances for $n = 15$ specimens present in the free environment and $n = 22$ specimens in the microfluidic channels. The resulting

p-values are reported in the corresponding paragraph. Statistical significance was determined as $p \leq 0.05$.

RESULTS

Viability and Developmental Steps of *Ectocarpus* Filaments Within the Lab-on-Chip

The early development of the *Ectocarpus* sporophyte has been described in detail (Le Bail et al., 2008, 2010, 2011; Nehr et al., 2011; Rabillé et al., 2019a) and is summarised in **Figure 3**. When grown in open space environments, the *Ectocarpus* sporophyte is composed of microscopic, branched uniseriate filaments (**Figure 3A**) that form a visible tuft approximatively 4 weeks after the very initial stages (**Figure 3B**). Sporophytic filaments growth is initiated by an asymmetrical cell division

of the zygote or mitospores (**Figure 3C**), forming the first apical cell that continues to grow indefinitely by tip growth (**Figure 3D**). A few hours later, the initial cell germinates again and gives rise to a second apical cell, which grows along the same axis as the first one but in the opposite direction. Over the span of several days, each first apical cell gradually differentiates into spherical cells. Apical growth and cell rounding generate a uniserial filament which is composed of two main cell types, i.e., elongated cells with a width of approximately 7 µm located at both ends of the filaments and circular cells with a diameter of approximately 15 µm situated at the centre of the filaments (**Figure 3E**). After around 10 days, the sub-apical cells branch (**Figure 3F**) and the resulting branches continue to grow as the primary filaments do. This repeated developmental programme results in the overall morphology as shown in **Figure 3B**.

FIGURE 3 | Morphology and development of *Ectocarpus* prostrate filaments. The general morphology of early **(A)** and later **(B)** prostrate filaments. **(C–F)** Schematic representations of the filament development and growth. **(C)** Zygotes, mitospores, or parthenogenetic gametes (all brown disks) germinate, divide asymmetrically (dashed line represents the germinating tube), and produce the first, highly polarised, apical cell. **(D)** Growth occurs at the tip of the apical cell and is indeterminate (arrow). It produces 7 µm wide cells. **(E)** The elongated, up to 60 µm long cylindrical apical cells progressively differentiate into rounder cells that are 15 µm wide. **(F)** In the meantime, branching takes place on the shank of sub apical cells (arrow). The branch re-iterates the same developmental pattern as the primary filament. Scale bars: **(A)** 100 µm; **(B)** 1 mm.

FIGURE 4 | Development of *Ectocarpus* filaments in PDMS lab-on-chips. **(A)** Germination and first division of spores after inoculation inside the lab-on-chip chamber. Spores divided mainly asymmetrically. **(B)** Apical cell growth. **(C)** Cell rounding at the centre of the filament. **(D)** Branching of the filaments. The lower image is taken from a device with 40 µm wide channels. Scale bars: 25 µm. All images were taken from lab-on-chips with 25 µm wide channels unless otherwise indicated.

We investigated whether these developmental steps were preserved in the constrained environment of the lab-on-chip devices. *Ectocarpus* spores were introduced into the structures as described in section "Materials and Methods." We monitored growth in the lab-on-chip with the goal of constraining the spores to germinate in the chamber. The spores successfully germinated inside the main chamber of the microfluidic device 5 days after inoculation (**Figure 4A**). The ratio of cell division asymmetry, i.e., the ratio of cell divisions producing unequally sized daughter cells as depicted in **Figure 3C**, was consistent with what was reported in open space germination, where about 80% of spores divide asymmetrically and approximately 20% symmetrically (Le Bail et al., 2011). When grown freely in water deprived of microelements, it has previously been observed that filaments tend to develop a cell sheet, meaning that *Ectocarpus* filaments shifted their development from uniaxial to bidirectional growth. This major change in body plan organisation is a sign that tip growth mechanisms have been severely impaired in the absence of microelements. However, in none of the lab-on-chips with 40 or 25 μm wide channels were such patterns observed and the filaments maintained an uniaxial growth throughout the experiment (**Figure 4B**) which indicates a sufficient supply of microelements even inside the confined regions of the lab-on-chip devices. Calcofluor staining further showed that filament growth took place in the dome of the apical cell (**Figure 5I**) as previously observed in open space environments (Le Bail et al., 2008). To monitor specimen health,

the growth rates of 22 filaments growing in 25 μm wide channels for 1 week were compared to the growth behaviour of filaments thriving in the open space environment of the same Petri dish (**Figures 6A,B**). **Figures 6C,D** showed that the overall growth dynamics were similar between the confined and free filaments, with filaments that grew inside the channels having an average growth rate of 2.8 $\mu m \cdot h^{-1}$ compared to 2.41 $\mu m \cdot h^{-1}$ for filaments growing in the open space (**Supplementary Table 1**; t-test p-value = 0.39). While the growth rates appeared to decrease with time independently of the environment (e.g., from 3.13 to 2.60 $\mu m \cdot h^{-1}$ inside the microchannels), this reduction in growth speed did not reach statistical significance (t-test p-value = 0.15). For direct comparisons, **Supplementary Figure 3** displays the average growth rate over time for both environments in a single graph. Overall, the observed growth rates occur with the same dynamic as previously reported, i.e., 2.5 $\mu m \cdot h^{-1}$ (Rabillé et al., 2019a).

The rounding of the cells is a function of their maturation stage and their position along the filament. It is, therefore, an excellent qualitative parameter reflecting the fitness of *Ectocarpus*. Rounding of elongated sub-apical cells (**Figure 3E**) was observed as expected, so that spherical cells were located only in the most proximal parts of the filaments (**Figure 4C**). Additionally, branching, which is an additional cellular event reflecting the canonical developmental pattern as described in **Figure 3**, also occurred in the filaments developed within the channels (**Figures 4C,D**). Furthermore, we did not notice any
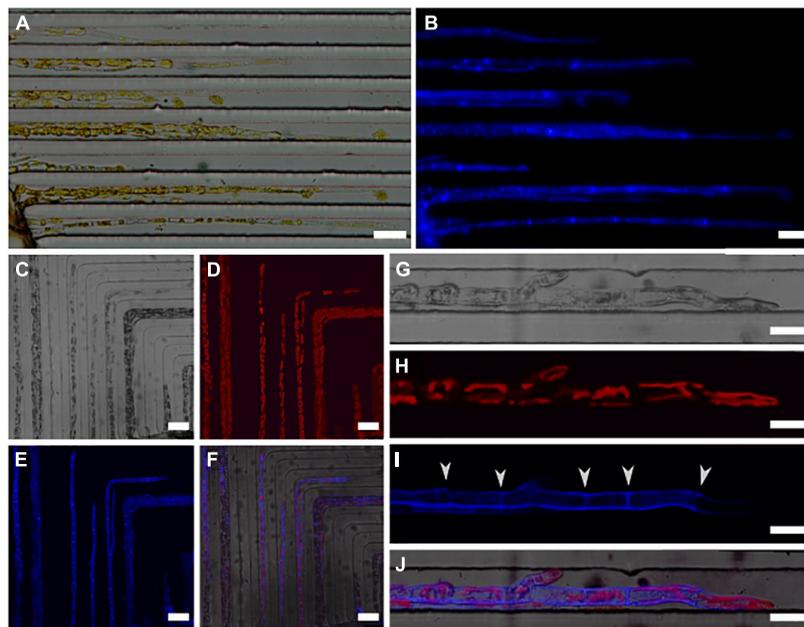
FIGURE 5 | Labelling of cellulose in the cell wall of filaments growing in 25 μm wide channels. **(A,B)** Two images obtained using epifluorescence microscopy. **(A)** A bright field microscopy image of the filaments and **(B)** a UV image showing the labelled cellulose (blue) present in the external cell wall. A stronger signal has been observed in the transversal walls. **(C–J)** A series of confocal microscopy images. **(C)** A bright field image of growing filaments, **(D)** chloroplast autofluorescence (red), **(E)** calcofluor fluorescence (blue), and **(F)** a merged image of all three channels. **(G,H)** A close-up of filaments labelled with calcofluor and imaged after growing for 24 h following the post-labelling rinsing of the channels. **(G)** The bright field image, **(H)** chloroplast fluorescence (red), **(I)** calcofluor fluorescence (blue), and **(J)** the three merged channels. The transverse cell walls (white arrowheads) are clearly distinguishable. The tip of the filament is not fluorescent, and as such, displays the newly grown cell wall. Scale bars: **(A–F)** 50 μm; **(G–J)** 25 μm.

FIGURE 6 | Growth rate of *Ectocarpus* filaments in lab-on-chip channels and in the open space. **(A,B)** Optical microscopy images of filaments growing in the open space environment, i.e., at the bottom of the Petri dish, as well as inside the lab-on-chip device. **(C,D)** The filament growth curves over three time points, i.e., at 24, 76, and 100 h after the first recording of the initial tip position. The initial tip position was set to 0 by default, such that the growth distance can be indicated through relative positions. The *p*-values for two-tailed *t*-tests for unequal variances are shown for each time point below **(D)**. Each line represents a single filament. The sample sizes for filaments growing in the open space environment and inside the channels are 15 and 22, respectively. The measurement data is reported in **Supplementary Table 1**. Scale bars: **(A,B)** 500 μm.

colour changes from brown to green in the chloroplasts of cells growing inside the microfluidic chip, which is typically observed in correlation with filament death. Finally, under UV exposure, the intensity of the auto-fluorescence emitted by the chloroplasts was detected at a level similar to that of filaments growing in the open space environment (see **Figures 5D,H**).

Therefore, for spores germinating inside the chamber, neither the presence of the PDMS nor the enforced space limitations demonstrated a negative effect on the filament development and growth pattern, e.g., by impairing the quality of the seawater inside the confined environment or through a possible increase in mechanical stress. Altogether, the developmental pattern of the filaments growing inside the channels, i.e., apical cell polarisation, growth rate, and cell shape changes, was consistent with the pattern observed in filaments growing in an open environment.

Display of Cellular Components of *Ectocarpus* Within the Lab-on-Chip

Despite the recent advances of editing approaches of *Ectocarpus* (Badis et al., 2021), the expression of fluorescent reporter genes is not yet feasible. Therefore, the study of *Ectocarpus* cell biology requires the use of classical cytological approaches, like vital staining and immunolocalisation that are the only available non-invasive techniques allowing for the labelling of specific components in or at the surface of the algal cells. Cellulose,

i.e., a rigid polymer of β(1–4) glucose present in *Ectocarpus* cell walls at a level of approximately 10% (Charrier et al., 2019), was uniformly labelled throughout filaments growing inside the 25 μm wide channels on both the outer and transverse cell walls (**Figures 5A,B**). This observation is in great agreement with previous studies for filaments grown in open space environment (Le Bail et al., 2008; Simeon et al., 2020). Similar results were also obtained for filaments in devices with 40 μm wide channels. Using confocal microscopy, the more focused images shown in **Figures 5C–F** confirmed the overall and homogeneous labelling of all filaments present inside channels. Both the shape of the chloroplasts highlighted by autofluorescence (**Figures 5G,H**) and the apical growth indicated by the new dark area at the filament tip (**Figures 5I,J**) confirmed that the filaments were thriving in this confined environment and, hence, supported the value of the previously derived growth rate measurements.

In a second step, we labelled alginates, i.e., a polysaccharide consisting of a mixture of guluronic and mannuronic acids linked by β(1–4) bond, which is present in brown algal cell walls at a ratio of up to 40% (reviewed in Charrier et al., 2019). The monoclonal BAM6, that recognises mannuronan-rich alginates, was used in combination with a secondary antibody coupled to the green fluorochrome FITC. The immunolocalisation protocol was applied in the lab-on-chip, aiming to label several filaments growing in parallel in separate channels. Simultaneously, free organisms present in the same Petri dish were labelled and used as positive controls. In contrast to the negative control without primary antibody (**Figures 7A–C**), the cell wall of both apical (**Figures 7D,E**) and rounding cells (**Figure 7F**) of labelled free-growing organisms displayed a specific signal similar to that reported in Rabillé et al. (2019b). In the 25 μm channels, *Ectocarpus* filaments also showed a strong signal in the dome of apical cells (**Figures 7G–J**) and on the flanks of rounding cells (**Figure 7K**). This pattern was as strong and specific as in the internal positive controls. The remaining cell walls of an empty plurilocular sporangium incidentally present within one of the channels also displayed significant labelling (**Figure 7L**). The red autofluorescence signal emitted by the chloroplasts further demonstrated the healthiness of the filaments prior to the formaldehyde fixation step of the immunolocalisation protocol (**Figures 7A–J**).

Overall, both cell biology protocols successfully labelled cellulose and alginate cell wall polysaccharides, either homogeneously (cellulose) or in specific locations (alginates) along the filaments. The labelling of the filaments was independent of the position of the specimen inside the lab-on-chip, e.g., at the entrance or exit of the channels, and displayed expected results even for samples located far away from the main chamber (**Figure 7G**).

DISCUSSION

Ectocarpus early development is accompanied by a significant number of cellular events while its morphological complexity is low. Initially, it leads to the formation of uniseriate filaments, which grow by elongation and division of apical cells, and
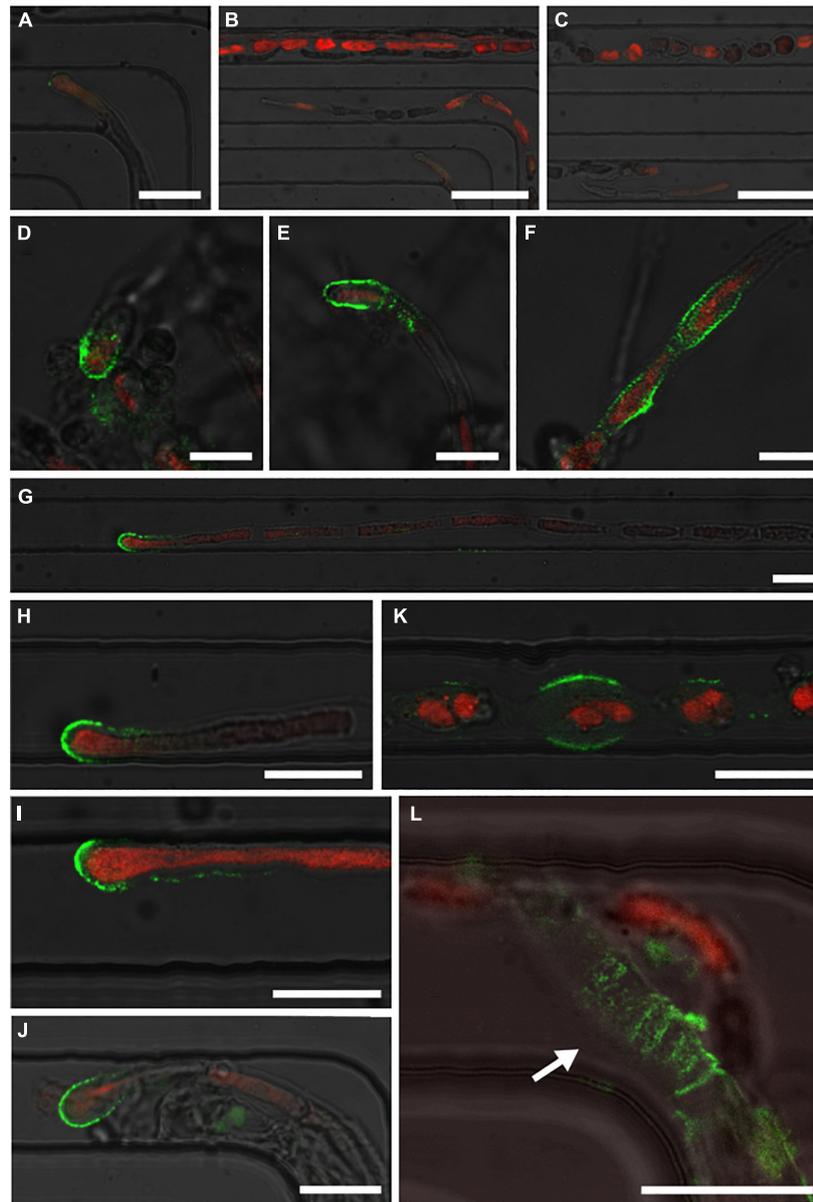
FIGURE 7 | Immunolocalisation of alginate polysaccharides in *Ectocarpus* filaments using monoclonal antibody BAM6. Labelled sections were observed through confocal microscopy. **(A–C)** Optical microscopy images demonstrating the negative controls for filaments without primary anti-alginate antibody. Both the apical parts and central parts of several filaments are shown without any signal from BAM6 (green fluorescent signal from the secondary FITC-conjugated antibody). Only autofluorescence (red) emitted by the chloroplasts was detected. **(D–F)** Optical images presenting freely growing filaments in the same Petri dish. With the same image capture parameters such as laser power and selective bands of the photomultiplier tubes, BAM6 labelling was observed in the dome of apical cells and in the flanks of rounded cells. **(G–L)** Image series showing the results on filaments grown in 25 μm wide channels. **(G–J)** Fluorescent images of the domes of apical cells, **(K)** rounding cells, and **(L)** empty plurilocular sporangium (white arrow). The autofluorescence of chloroplasts of BAM6 labelled filaments was observed, except in **L**, as the cavities of the plurilocular sporangium no longer contained spores. Scale bars: **(A)** 25 μm; **(B,C)** 50 μm; **(D–F)** 10 μm; **(G–L)** 20 μm. The specific green BAM6 signal and the red chloroplast autofluorescence signals are superimposed with the bright field signal.

the progressive rounding of cells acting as the main cell differentiation process. Recently, it has been demonstrated that *Ectocarpus* tip growth relies on a different biophysical mechanism than that reported in most of the other tip growing cells, including the pollen tube. In the former, the cell wall stiffness controls growth (Rabillé et al., 2019a), while in the latter, this

is the cell wall thickness. This further illustrated that brown algae are promising model organisms to display alternative growth mechanisms.

To study the tip growth behaviour of *Ectocarpus*, we tested the use of lab-on-chips as a microfluidic device aimed for the long-term monitoring of filaments. The possibility of delivering

chemicals at a specific time and simultaneously to several filaments growing in a single focal plane while being guided through parallel channels is particularly attractive for slow growing specimens such as the *Ectocarpus* filaments. Here, we have shown that microfluidic chips with 44 parallel channels as narrow as 25 μm are suitable for studying *Ectocarpus* tip growth and dynamics of cell rounding. The inoculation procedure and cell wall labelling experiments were developed such that more than 50% of the lab-on-chip channels were filled with healthy filaments growing in-plane over more than 3 weeks, which is a duration that significantly exceeds the typical use of such technology for other samples (Agudelo et al., 2013; Shamsudhin et al., 2016; Burri et al., 2018). Furthermore, the presented designs allowed for the incorporation of specimen studies using standard cytology protocols. Our observations are consistent with previous conclusions drawn for the protonemata of the moss *P. patens*, where the growth rate and cell differentiation, with some impairments (Kozgunova and Goshima, 2019), proceeded as expected (Bascom et al., 2016). In contrast, different results were obtained with the hyphae of the fungi *N. crassa* growing in grid or maze chips, where the velocity of the apical extension was drastically reduced and their branching pattern impaired (Held et al., 2011).

In our case, possible limitations depended on the applied loading procedure and the inoculation of the mitospores. While the filaments successfully entered and grew along the microchannels if the mitospores were germinated in the main chamber, mitospores loaded inside the channels were severely hindered in their germination. However, by optimising the inoculation procedure, we were able to prevent these drawbacks. Furthermore, the study of germination and especially of the first asymmetric cell division did not rely on a specific device geometry as both major cellular events could be observed in all spatial directions. Altogether, this study validates the use of microfluidic devices for the study of the development and of the physiology of *Ectocarpus* in a confined microenvironment. Hence, it represents a first step in the subsequent characterisation of tip growing mutants (Le Bail et al., 2011) and potentially life cycle mutants of this species (Coelho et al., 2011; Macaisne et al., 2017), as it has previously been performed with *Physcomitrium* (Bascom et al., 2016) and *Neurospora* (Held et al., 2011). It also paves the way for the study of other brown algae, especially those which develop filaments in one or both phases of their life cycle, such as *Sphacelaria* and filamentous gametophytes of many brown algae including the Laminariales, the Desmarestiales, and the Sporochnales (Fritsch, 1954).

CONCLUSION

In recent years, microfluidic devices have proven suitable for the investigation and manipulation of numerous small organisms and, by that, enabled novel possibilities and pathways for biological research. However, prior to their application, lab-on-chips must first be evaluated for each potential biological model to avoid misinterpretations of newly gained observations and of the corresponding results. In this work, the healthiness

and performance of *Ectocarpus* filaments growing in confined microfluidic environments were monitored under controlled conditions for several days and the development steps were quantitatively and qualitatively compared to *in vitro* open space growth. Additionally, the ability to label cytological markers, either by immunochemistry or directly with vital dyes, was investigated to ensure the suitability of microfluidic devices for the in-depth study of the brown alga *Ectocarpus*. The results demonstrated that, following an optimised loading procedure, all the developmental steps of *Ectocarpus* filament growth inside PDMS channels were similar to those observed in unconstrained conditions and as described in previous reports. Therefore, PDMS lab-on-chips are suitable experimental devices to further study apical growth, cell differentiation, and branching and enable simplified investigations by allowing for chemically controlled environments in combination with high-resolution microscopy techniques.

DATA AVAILABILITY STATEMENT

The raw data supporting the conclusions of this article will be made available by the authors, without undue reservation.

AUTHOR CONTRIBUTIONS

BC and NL conceived the initial idea and wrote the manuscript. BC and BN supervised the project. BC, BN, and NL raised the funding. NL designed and fabricated the microfluidic devices. BC adjusted the culture conditions and monitored growth. SB performed the cell wall staining experiments. All authors reviewed and commented on the manuscript.

FUNDING

ACKNOWLEDGMENTS

SUPPLEMENTARY MATERIAL

The Supplementary Material for this article can be found online at: https://www.frontiersin.org/articles/10.3389/fmars.2021.745654/full#supplementary-material

REFERENCES

Agudelo, C., Packirisamy, M., and Geitmann, A. (2016). Influence of electric fields and conductivity on pollen tube growth assessed via electrical lab-on-chip. *Sci. Rep.* 6:19812. doi: 10.1038/srep19812

Agudelo, C. G., Nezhad, A. S., Ghanbari, M., Naghavi, M., Packirisamy, M., and Geitmann, A. (2013). TipChip: a modular, MEMS-based platform for experimentation and phenotyping of tip-growing cells. *Plant J.* 73, 1057–1068. doi: 10.1111/tpj.12093

Azizipour, N., Avazpour, R., Rosenzweig, D. H., Sawan, M., and Ajji, A. (2020). Evolution of biochip technology: a review from lab-on-a-chip to organ-on-a-chip. *Micromachines* 11:599. doi: 10.3390/mi1106 0599

Badis, Y., Scornet, D., Harada, M., Caillard, C., Godfroy, O., Raphalen, M., et al. (2021). Targeted CRISPR-Cas9-based gene knockouts in the model brown alga *Ectocarpus*. *New Phytol.* 231, 2077–2091. doi: 10.1111/nph. 17525

Baldauf, S. L. (2003). The deep roots of eukaryotes. *Science* 300, 1703–1706. doi: 10.1126/science.1085544

Bascom, C. S., Wu, S.-Z., Nelson, K., Oakey, J., and Bezanilla, M. (2016). Long-term growth of moss in microfluidic devices enables subcellular studies in development. *Plant Physiol.* 172, 28–37. doi: 10.1104/pp.16. 00879

Bayareh, M., Ashani, M. N., and Usefian, A. (2020). Active and passive micromixers: a comprehensive review. *Chem. Eng. Process. Process Intensification* 147:107771. doi: 10.1016/j.cep.2019. 107771

Berlanda, S. F., Breitfeld, M., Dietsche, C. L., and Dittrich, P. S. (2021). Recent advances in microfluidic technology for bioanalysis and diagnostics. *Anal. Chem.* 93, 311–331. doi: 10.1021/acs.analchem.0c04366

Bogaert, K. A., Blommaert, L., Ljung, K., Beeckman, T., and De Clerck, O. (2019). Auxin function in the brown alga *Dictyota dichotoma*. *Plant Physiol.* 179, 280–299. doi: 10.1104/pp.18.01041

Bothwell, J. H. F., Kisielewska, J., Genner, M. J., McAinsh, M. R., and Brownlee, C. (2008). Ca2+ signals coordinate zygotic polarization and cell cycle progression in the brown alga *Fucus serratus*. *Dev. Camb. Engl.* 135, 2173–2181. doi: 10. 1242/dev.017558

Burri, J. T., Vogler, H., Läubli, N. F., Hu, C., Grossniklaus, U., and Nelson, B. J. (2018). Feeling the force: how pollen tubes deal with obstacles. *New Phytol.* 220, 187–195. doi: 10.1111/nph.15260

Charrier, B., Coelho, S. M., Le Bail, A., Tonon, T., Michel, G., Potin, P., et al. (2008). Development and physiology of the brown alga *Ectocarpus siliculosus*: two centuries of research. *New Phytol.* 177, 319–332. doi: 10.1111/j.1469-8137. 2007.02304.x

Charrier, B., Rabillé, H., and Billoud, B. (2019). Gazing at cell wall expansion under a golden light. *Trends Plant Sci.* 24, 130–141. doi: 10.1016/j.tplants.2018. 10.013

Cock, J. M., Sterck, L., Rouzeé, P., Scornet, D., Allen, A. E., Amoutzias, G., et al. (2010). The *Ectocarpus* genome and the independent evolution of multicellularity in brown algae. *Nature* 465, 617–621. doi: 10.1038/nature 09016

Coelho, S. M., Godfroy, O., Arun, A., Le Corguillé, G., Peters, A. F., and Cock, J. M. (2011). OUROBOROS is a master regulator of the gametophyte to sporophyte life cycle transition in the brown alga *Ectocarpus*. *Proc. Natl. Acad. Sci. U.S.A.* 108, 11518–11523. doi: 10.1073/pnas.1102274108

Evariste, E., Gachon, C. M. M., Callow, M. E., and Callow, J. A. (2012). Development and characteristics of an adhesion bioassay for ectocarpoid algae. *Biofouling* 28, 15–27. doi: 10.1080/08927014.2011.643466

Fritsch, F. E. (1954). *The Structure and Reproduction of the Algae*, Vol. II. Cambridge: Cambridge University Press.

Held, M., Edwards, C., and Nicolau, D. V. (2011). Probing the growth dynamics of *Neurospora crassa* with microfluidic structures. *Fungal Biol.* 115, 493–505. doi: 10.1016/j.funbio.2011.02.003

Kozgunova, E., and Goshima, G. (2019). A versatile microfluidic device for highly inclined thin illumination microscopy in the moss *Physcomitrella patens*. *Sci. Rep.* 9:15182. doi: 10.1038/s41598-019-51624-9

Läubli, N. F., Burri, J. T., Marquard, J., Vogler, H., Mosca, G., Vertti-Quintero, N., et al. (2021a). 3D mechanical characterization of single cells and small organisms using acoustic manipulation and force microscopy. *Nat. Commun.* 12:2583. doi: 10.1038/s41467-021-22718-8

Läubli, N. F., Gerlt, M. S., Wüthrich, A., Lewis, R. T. M., Shamsudhin, N., Kutay, U., et al. (2021b). Embedded microbubbles for acoustic manipulation of single cells and microfluidic applications. *Anal. Chem.* 93, 9760–9770. doi: 10.1021/ acs.analchem.1c01209

Le Bail, A., Billoud, B., Kowalczyk, N., Kowalczyk, M., Gicquel, M., Le Panse, S., et al. (2010). Auxin metabolism and function in the multicellular brown alga *Ectocarpus siliculosus*. *Plant Physiol.* 153, 128–144. doi: 10.1104/pp.109. 149708

Le Bail, A., Billoud, B., Le Panse, S., Chenivesse, S., and Charrier, B. (2011). ETOILE regulates developmental patterning in the filamentous brown alga *Ectocarpus siliculosus*. *Plant Cell* 23, 1666–1678. doi: 10.1105/tpc.110. 081919

Le Bail, A., Billoud, B., Maisonneuve, C., Peters, A., Cock, J. M., and Charrier, B. (2008). Initial pattern of development of the brown alga *Ectocarpus siliculosus* (Ectocarpales: Phaeophyceae) sporophyte. *J. Phycol.* 44, 1269–1281.

Le Bail, A., and Charrier, B. (2013). "Culture methods and mutant generation in the filamentous brown algae *Ectocarpus siliculosus*," in *Plant Organogenesis Methods in Molecular Biology*, ed. I. De Smet (Totowa, NJ: Humana Press), 323–332. doi: 10.1007/978-1-62703-221-6_22

Macaisne, N., Liu, F., Scornet, D., Peters, A. F., Lipinska, A., Perrineau, M.-M., et al. (2017). The *Ectocarpus* immediate upright gene encodes a member of a novel family of cysteine-rich proteins with an unusual distribution across the eukaryotes. *Development* 144, 409–418. doi: 10.1242/dev.14 1523

Michel, G., Tonon, T., Scornet, D., Cock, J. M., and Kloareg, B. (2010). Central and storage carbon metabolism of the brown alga *Ectocarpus siliculosus*: insights into the origin and evolution of storage carbohydrates in eukaryotes. *New Phytol.* 188, 67–81. doi: 10.1111/j.1469-8137.2010. 03345.x

Nehr, Z., Billoud, B., Le Bail, A., and Charrier, B. (2011). Space-time decoupling in the branching process in the mutant étoile of the filamentous brown alga *Ectocarpus siliculosus*. *Plant Signal. Behav.* 6, 1889–1892.

Pei, H., Li, L., Han, Z., Wang, Y., and Tang, B. (2020). Recent advances in microfluidic technologies for circulating tumor cells: enrichment, single-cell analysis, and liquid biopsy for clinical applications. *Lab Chip* 20, 3854–3875. doi: 10.1039/d0lc00577k

Peyrin, J. M., Deleglise, B., Saias, L., Vignes, M., Gougis, P., Magnifico, S., et al. (2011). Axon diodes for the reconstruction of oriented neuronal networks in microfluidic chambers. *Lab Chip* 11, 3663–3673. doi: 10.1039/c1lc2 0014c

Popper, Z. A., Michel, G., Hervé, C., Domozych, D. S., Willats, W. G. T., Tuohy, M. G., et al. (2011). Evolution and diversity of plant cell walls: from algae to flowering plants. *Annu. Rev. Plant Biol.* 62, 567–590. doi: 10.1146/annurev-arplant-042110-103809

Rabillé, H., Billoud, B., Tesson, B., Le Panse, S., Rolland, É., and Charrier, B. (2019a). The brown algal mode of tip growth: keeping stress under control. *PLoS Biol.* 17:e2005258. doi: 10.1371/journal.pbio.2005258

Rabillé, H., Torode, T. A., Tesson, B., Le Bail, A., Billoud, B., Rolland, E., et al. (2019b). Alginates along the filament of the brown alga *Ectocarpus* help cells cope with stress. *Sci. Rep.* 9:12956. doi: 10.1038/s41598-019-49427-z

Shamsudhin, N., Laeubli, N., Atakan, H. B., Vogler, H., Hu, C., Haeberle, W., et al. (2016). Massively parallelized pollen tube guidance and mechanical measurements on a lab-on-a-chip platform. *PLoS One* 11:e0168138. doi: 10. 1371/journal.pone.0168138

Siddique, R., and Thakor, N. (2013). Investigation of nerve injury through microfluidic devices. *J. R. Soc. Interface* 11:20130676. doi: 10.1098/rsif.2013. 0676

Simeon, A., Kridi, S., Kloareg, B., and Herve, C. (2020). Presence of exogenous sulfate is mandatory for tip growth in the brown alga *Ectocarpus subulatus*. *Front. Plant Sci.* 11:1277. doi: 10.3389/fpls.2020.01277

Tong, Z., Segura-Feliu, M., Seira, O., Homs-Corbera, A., Del Río, J. A., and Samitier, J. (2015). A microfluidic neuronal platform for neuron axotomy and controlled regenerative studies. *RSC Adv.* 5, 73457–73466. doi: 10.1039/ c5ra11522a

Zhou, X., Lu, J., Zhang, Y., Guo, J., Lin, W., Norman, J. M. V., et al. (2021). Membrane receptor-mediated mechano-transduction maintains cell integrity during pollen tube growth within the pistil. *Dev. Cell* 56, 1030–1042.e6. doi: 10.1016/j.devcel.2021.02.030

Zhu, H., Fohlerova, Z., Pekarek, J., Basova, E., and Neuzil, P. (2020). Recent advances in lab-on-a-chip technologies for viral diagnosis. *Biosens. Bioelectron.* 153:112041. doi: 10.1016/j.bios.2020.11 2041

Conflict of Interest: The authors declare that the research was conducted in the absence of any commercial or financial relationships that could be construed as a potential conflict of interest.